# Structure-Based Discovery of Novel Non-nucleosidic DNA Alkyltransferase Inhibitors: Virtual Screening and in Vitro and in Vivo Activities

Federico M. Ruiz,[†] Rubén Gil-Redondo,[‡] Antonio Morreale,[‡] Ángel R. Ortiz,*[,‡] Carmen Fábrega,*[,†] and Jerónimo Bravo*[,†]

Signal Transduction Group, Structural Biology and Biocomputing Programme, Centro Nacional de Investigaciones Oncológicas (CNIO), Melchor Fernández Almagro 3, E-28029 Madrid, Spain, and Bioinformatics Unit, Centro de Biología Molecular Severo Ochoa (CSIC-UAM), Universidad Autónma de Madrid, Nicolás Cabrera, 1. Cantoblanco, 28049 Madrid, Spain

Received November 30, 2007

The human DNA-repair $O^6$-alkylguanine DNA alkyltransferase (MGMT or hAGT) protein protects DNA from environmental alkylating agents and also plays an important role in tumor resistance to chemotherapy treatment. Available inhibitors, based on pseudosubstrate analogs, have been shown to induce substantial bone marrow toxicity in vivo. These deficiencies and the important role of MGMT as a resistance mechanism in the treatment of some tumors with dismal prognosis like glioblastoma multiforme, the most common and lethal primary malignant brain tumor, are increasing the attention toward the development of improved MGMT inhibitors. Here, we report the identification for the first time of novel non-nucleosidic MGMT inhibitors by using docking and virtual screening techniques. The discovered compounds are shown to be active in both in vitro and in vivo cellular assays, with activities in the low to medium micromolar range. The chemical structures of these new compounds can be classified into two families according to their chemical architecture. The first family corresponds to quinolinone derivatives, while the second is formed by alkylphenyl-triazolo-pyrimidine derivatives. The predicted inhibitor protein interactions suggest that the inhibitor binding mode mimics the complex between the excised, flipped out damaged base and MGMT. This study opens the door to the development of a new generation of MGMT inhibitors.

In spite of the considerable progress in cancer cell biology, most cancer treatments are still multimodal, involving extensive surgery, radiotherapy, and chemotherapy treatment. Chemotherapy remains the most important pharmacological approximation to cancer therapy. Cytotoxic alkylating agents (e.g., streptozotocin, procarbazine, or dacarbazine) are the oldest family of anticancer drugs.[1] The sites of reaction of alkylating agents in guanine include $N^1$, $N^3$, $N^7$, and $O^6$. The $N^7$ position is the most reactive site,[2–4] however the DNA functions are most strongly affected by alkylation in the $O^6$ position.[5] 1,3-Bis-(2-chloroethyl)-1-nitrosourea (BCNU) attacks initially at the $O^6$ guanine position followed by formation of a cyclic intermediate with attack at the $N^1$ position of guanine, giving rise to $N^1O^6$ ethanoguanine. Finally the structure rearranges from the O to form a cross-link with the opposite cytosine.[6] Eventually, DNA replication is blocked, producing G2/M rest.[7] In addition to the well-known side effects and limitations of chemotherapeutic agents, they also present problems of acquired tumor resistance. Particularly, the human DNA-repair $O^6$-alkylguanine DNA alkyltransferase (MGMT or hAGT), an important protein that protects DNA from environmental alkylating agents, also plays an important role as a resistance mechanism. It is well established that resistance to both chloroethylating and methylating chemotherapeutic agents and cyclophosphamide (a nitrogen mustard alkylating agent) is mediated by MGMT activity,[8–11] as tumor cells frequently express high levels of this enzyme. This effect has been observed in a number of cancers, ranging from colon cancer, lung tumors, breast cancer, pancreatic tumors and non-Hodgkin's lymphomas to myelomas and gliomas, among others.[12–14] It is significant that MGMT promoter methylation, and consequently complete MGMT depletion, has been statistically associated with longer survival in patients with high grade gliomas under radiation-chemotherapy combined treatment.[15,16] Pharmacological inhibition of MGMT, therefore, has the potential to enhance the cytotoxic effect of a diverse range of anticancer agents, particularly in colon and brain tumors.

Despite pharmacological interest and the efforts in the structural biology of DNA repair, the first two structures of MGMT-damaged DNA have only been published recently.[17] These structures, an inactive C145S mutant bound to an $O^6$-methylguanine-containing oligonucleotide and an active MGMT covalently cross-linked to an oligonucleotide containing $N^1$,$O^6$-ethonaxanthosine, provided both, novel protein-DNA architecture and the structural basis for the reaction mechanism. The DNA-binding helix-turn-helix (HTH) motif is placed in the MGMT C-terminal domain of this 22 kDa protein (207 AA) with a two-domain $\alpha/\beta$ fold.[18] The second helix of this motif binds deep within the DNA minor groove. MGMT binds without changes but widening the minor groove and therefore bending the DNA. Arg128 is positioned

* To whom correspondence should be addressed. Tel.: 34-912246900 (C.F. and J.B.); 34-911964633 (A.R.O.). Fax: 34-912246976 (C.F. and J.B.); 34-911964420 (A.R.O). E-mail: cfabrega@cnio.es (C.F.); jbravo@cnio.es (J.B.); aro@cbm.uam.es (A.R.O.).
[†] Centro Nacional de Investigaciones Oncológicas (CNIO).
[‡] Centro de Biologia Molecular Severo Ochoa (CSIC-UAM).

10.1021/ci700447r CCC: $40.75 
Published on Web 03/20/2008

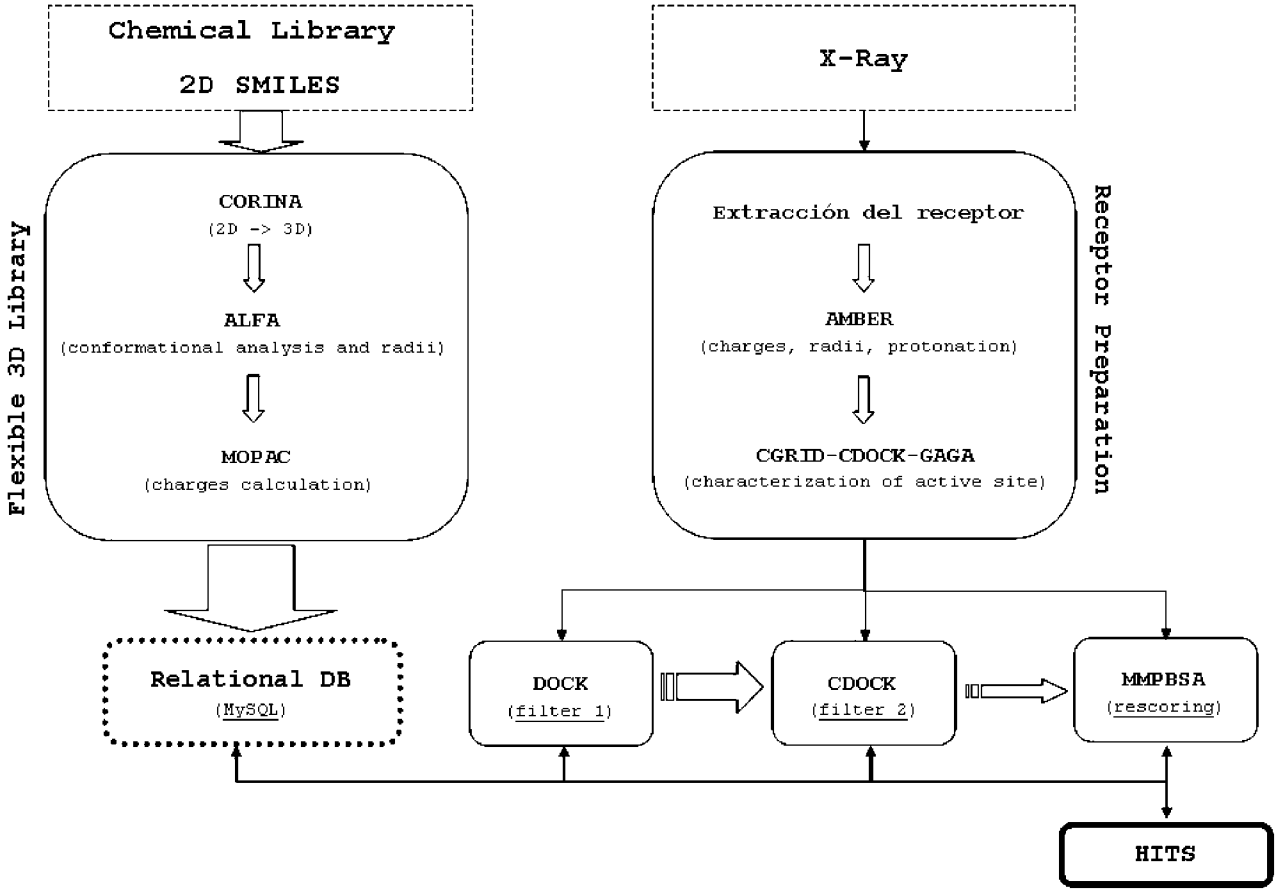


**Figure 1.** Flowchart of the virtual screening procedure applied in this work. See the main text for details.

inside the DNA duplex, stabilizing the structure by hydrogen bonds with the orphaned cytosine. This 'arginine finger,' also seems to promote the flipping of nucleotides out from the base stack, and into the MGMT hydrophobic active site. The observation that MGMT activity is decreased more than 1000 times when Arg128 is replaced by alanine confirms the essential role played by this residue.[19]

The nucleophilic residue, Cys145, is buried deeply into the active site, near the bottom of the hydrophobic active site pocket. This residue participates in a hydrogen bond network involving His146, Glu172, and a water molecule, which may act as a relay able to increase cysteine reactivity upon substrate binding. In the proposed enzymatic mechanism, His146 acts as a water-mediated base to deprotonate Cys145, which receives the alkyl lesion in a SN2 manner.[20] The DNA is restored but the protein, acting as a suicidal enzyme, inactivates itself in the process. Finally, the alkylated protein is destabilized,[21] recognized by an E3 ubiquitin ligase with its associated E2 ubiquitin-conjugating enzyme and degraded by an ATP-dependent pathway.[22,23]

Several small molecules acting as MGMT inhibitors have been developed during the past few years, all of them pseudosubstrates. The guanine analogue $O^6$-methylguanine ($O^6$-MG) was the first inhibitor discovered. It reduces MGMT activity in cells; however, it is not effective enough to be used in animal or clinical assays. A more rapid and effective depletion of MGMT was obtained with $O^6$-benzylguanine ($O^6$-BG).[24] $O^6$-BG acts as an alternative substrate for MGMT, transferring the benzyl group to the Cys145 and irreversibly inactivating the protein.[25] It has an $IC_{50}$ value of 0.2 $\mu$M against MGMT,[26] significantly enhancing the cytotoxic effect of BCNU in prostate, breast, colon and lung tumor cells[27] and in tumor xenograft studies.[28] Several phase I and II clinical studies of the combination of $O^6$-BG and BCNU have been completed.[29] However, significant therapeutic limitations have been observed: $O^6$-BG has low bioavailability, poor water solubility and rapid plasma clearance.[30] There is no evidence of toxicity associated to $O^6$-BG alone, however, when combined with BCNU, it increases myelo-suppression.[31,32] In addition, repeated administration of $O^6$-BG with BCNU raises the possibility of developing $O^6$-BG-resistantance. A point mutation in Lys165 has been associated with acquired $O^6$-BG and BCNU resistance in MMR-deficient medulloblastoma cell lines.[33] Direct evidence of the relation between Lys165 mutation and BCNU activity has been shown in MMR-deficient colon cancer cells.[34] In contrast MGMT independent resistance to $O^6$-BG has been found in breast cancer cells after treatment with this MGMT inhibitor plus BCNU.[35] Recently different guanine derivatives have been used in MGMT inhibition studies. Among them, lomeguatrib [6-(4-bromo-2-thienyl) methoxy]purin-2-amine] is more active in vitro than $O^6$-BG, having an $IC_{50}$ value of 0.018 $\mu$M.[34] This $O^6$-thenyl analogue of $O^6$-BG has been selected for clinical experiments and successfully used in combination with Temozolomide in a first phase I trial.[36]

Searching for new molecules has become in one of the most actives areas in computational chemistry and biology. Virtual screening protocols are being used routinely in this regard and there are many successful cases where

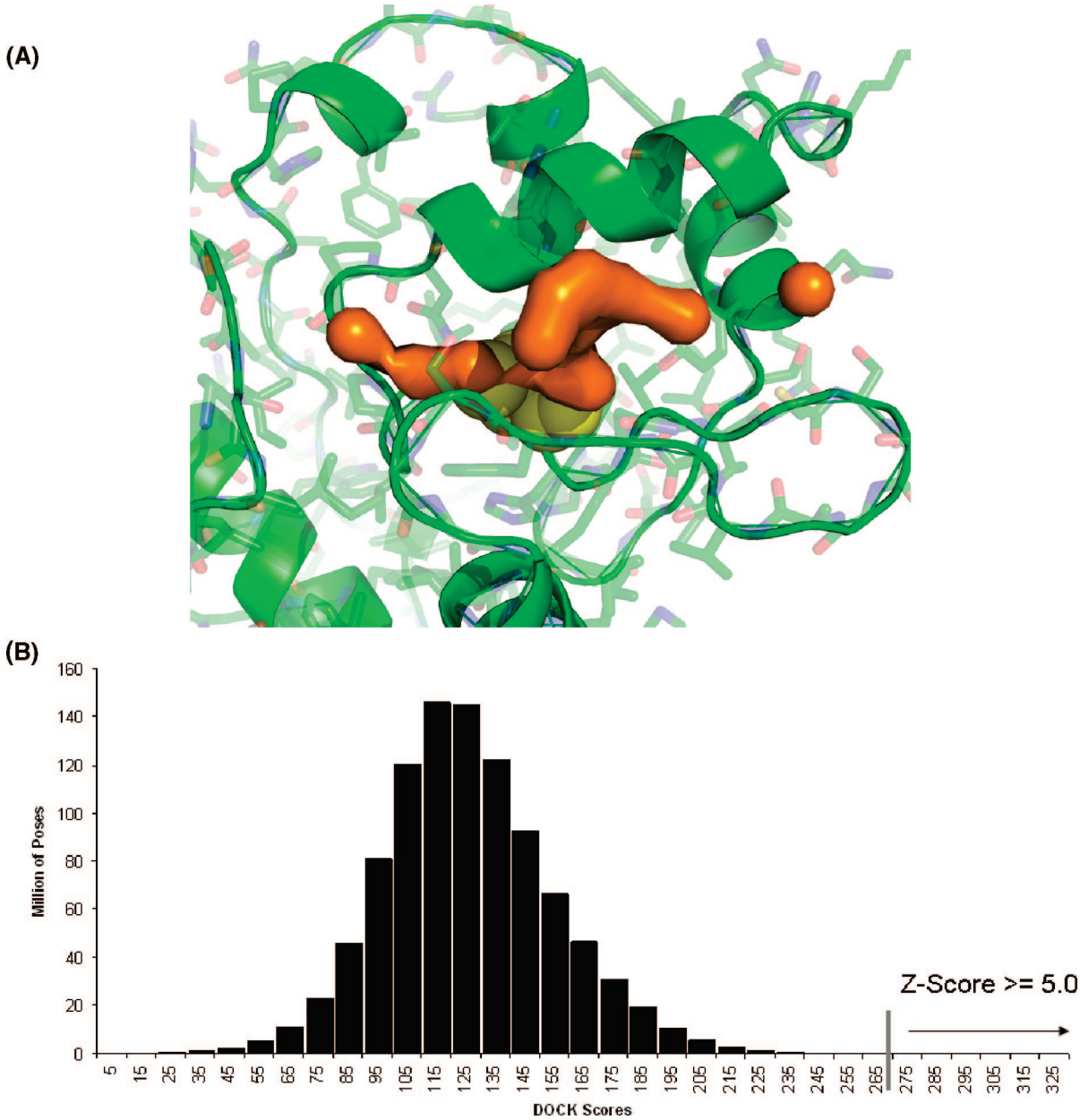


**Figure 2.** (A) Negative spheres image of the MGMT active site computed with GAGA. (B) DOCK score distribution showing the Zscore cutoff value applied.

novel inhibitors have been found.[37,38] The underlying engine that moves virtual screening consists of two pieces: a docking algorithm to sample the binding site of a receptor target, and a mathematical scoring function to assign a score to each binding site pose.[39] Usually, only the best solution for each molecule, the lowest in energy, is considered. With the advent of supercomputer virtual screening of chemical libraries is becoming a feasible issue, and it is customary to screen thousands or even millions of molecules in some virtual experiments. Screening such a large number of molecules comes with the problem that extremely large amount of time is required, and then accuracy is reduced to maintain time in a reasonable range. Accordingly, the receptor is kept rigid along the experiment, environmental effects (mainly due to solvent) are complete ignored or treated at a very low theoretical level, entropic effect are rarely taken into account. These shortcomings are often alleviated by post processing the highest ranked candidates (between 50 and 100) to more elaborated protocols as molecular dynamics simulations.[40,41] Then, selected snapshots from these trajectories are treated with approximations as MMPBSA,[42] MMGBSA,[43] or LIE[44] among others, to obtain an estimation of the free energy of binding, a measure comparable with experimental inhibition constants.

Motivated by the deficiencies of known inhibitors and the important role of MGMT in difficult tumors like gliomastoma multiforme (the most common and lethal primary malignant brain tumor), we report here the identification, for the first time, of novel non-nucleosidic MGMT inhibitors. Docking and virtual screening techniques, followed by molecular mynamics simulations and free energy of binding calculation with MMGBSA method yielded four promising compounds with experimental probed activities both in vitro and in vivo.

**Table 1.** List of the 17 Top-Ranked Compounds Obtained in the Virtual Screening Computation[a]

| | compound (ZINC code) | log P | H-bond donors | H-bond acceptors | charge | MW[b] | CDOCK energy | MMGBSA energy[c] | $IC_{50}$ ($\mu$M)[d] | $IC_{50}$ ($\mu$M)[e] |
|---|---|---|---|---|---|---|---|---|---|---|
| 1 | (ZINC00910802) | 3.52 | 2 | 9 | 1 | 536 | −34.57 | −32.26 (2.59) | 54 | 10 |
| 2 | (ZINC00889422) | 4.24 | 2 | 7 | 1 | 505 | −31.91 | −43.54 (3.35) | 34 | 50 |
| 3 | (ZINC03642335) | 6.18 | 1 | 5 | 0 | 410 | −32.42 | −46.52 (3.26) | 24 | 10 |
| 4 | (ZINC02487935) | 5.61 | 1 | 6 | 0 | 426 | −32.37 | −56.90 (3.24) | 22 | 10 |
| 5 | (ZINC01327643) | 4.23 | 2 | 6 | 0 | 437 | −31.24 | ND[f] | >100 | ND |
| 6 | (ZINC00714917) | 6.41 | 1 | 6 | 0 | 503 | −31.84 | ND | >100 | ND |
| 7 | (ZINC01360953) | 5.01 | 0 | 7 | 0 | 563 | −32.06 | ND | >100 | ND |
| 8 | (ZINC01360953) | 4.51 | 2 | 6 | 0 | 433 | −31.73 | ND | >100 | ND |
| 9 | (ZINC02809317) | 1.34 | 0 | 11 | 0 | 463 | −32.95 | ND | >100 | ND |
| 10 | (ZINC03404767) | 4.88 | 1 | 8 | 0 | 481 | −34.08 | ND | >100 | ND |
| 11 | (ZINC01437200) | 2.81 | 2 | 8 | 2 | 479 | −32.71 | ND | >100 | ND |
| 12 | (ZINC03052303) | 3.50 | 2 | 7 | 0 | 516 | −33.90 | ND | >100 | ND |
| 13 | (ZINC00784955) | 0.90 | 3 | 9 | 2 | 452 | −32.61 | ND | >100 | ND |
| 14 | (ZINC00892609) | 4.45 | 2 | 7 | 1 | 505 | −31.56 | ND | >100 | ND |
| 15 | (ZINC01352201) | 3.06 | 1 | 9 | 0 | 472 | −33.19 | ND | >100 | ND |
| 16 | (ZINC02835223) | 4.34 | 1 | 6 | 0 | 433 | −28.35 | ND | >100 | ND |
| 17 | (ZINC00738815) | 4.48 | 2 | 6 | 0 | 460 | −32.52 | ND | >100 | ND |

[a] The computed chemical properties (as found in the ZINC database), the computed binding energies (computed both with CDOCK and the MMGBSA method, see Materials and Methods for details), and the in vitro and in vivo activities of the active compounds are shown. [b] MW molecular weight. [c] Average interaction energy during the MD simulation in kilocalories per mole; standard deviation is shown in parenthesis. [d] $IC_{50}$ in vitro value (concentration of the compounds required to produce 50% reduction in the MGMT activity). [e] $IC_{50}$ in vivo value (concentration of the compounds required to produce 50% cell killing in the presence of 80 $\mu$M sBCNU). [f] ND not determined.

**Table 2.** Interaction Energy Analysis (Standard Deviations in Parentheses), As Computed from the Molecular Dynamics Simulations by the MMGBSA Approach, for the Four Active Molecules Found in This Work[a]

| | compound | | | |
|---|---|---|---|---|
| res no. | **1** | **2** | **3** | **4** |
| ARG128 | −5.99 (0.65) | −4.09 (1.51) | −6.01 (0.99) | −6.71 (0.64) |
| TYR114 | −1.92 (0.31) | −4.33 (0.47) | −5.46 (0.65) | −4.87 (0.46) |
| ARG135 | −5.52 (0.77) | −1.39 (0.56) | −3.51 (0.84) | −4.75 (0.95) |
| TYR158 | −1.53 (0.44) | −3.17 (0.41) | −1.39 (0.24) | −4.03 (0.55) |
| GLY131 | | −2.31 (0.44) | −2.83 (0.36) | −3.17 (0.38) |
| ASN157 | −2.69 (0.65) | −3.34 (0.42) | −1.38 (0.27) | −2.93 (0.52) |
| MET134 | | −3.11 (0.51) | −2.25 (0.34) | −2.58 (0.41) |
| ALA127 | −1.11 (0.24) | | | −1.68 (0.29) |
| SER159 | −1.30 (0.29) | −1.65 (0.35) | | −1.55 (0.29) |
| GLN115 | | | −2.36 (0.62) | −1.37 (0.33) |
| CYS150 | | | | −1.18 (0.46) |
| CYS145 | | −1.21 (0.32) | | −1.01 (0.42) |
| **total** | **−20.06 (0.48)** | **−24.60 (0.54)** | **−25.19 (0.51)** | **−35.83 (0.48)** |

[a] All values are in kilocalories per mole.

## RESULTS AND DISCUSSION

**Virtual Screening (VS).** The virtual screening protocol employed is summarized in Figure 1. and briefly described in the Materials and Methods section. An essential part in the procedure is to characterize the shape of the active site. For this we use our algorithm GAGA (see Materials and Methods) to obtain a negative image of the binding site (see Figure 2A). It can be seen that it covers the active site pocket and protrudes toward the neighborhood of Tyr114. Overall, the shape of the negative image resembles the shape of the target nucleotide bound to MGMT. Upon charactering the binding site, a library of 2.3 million compounds was screened. Compounds were first filtered with DOCK[45] using the negative image of the binding site as computed with GAGA. We chose to employ a Zscore (see Materials and Methods) cutoff value of 5 in the filtering step. From the initial set of 2.3 million of molecules, 1664 passed the ZScore cut off (Figure 2B). These molecules were then further screened with the CDOCK program, our in-house docking program. The CDOCK energies, computed with the CGRID molecular mechanics energy function, were solvent corrected in order to obtain the final scoring (see Materials and Methods). From the highest scoring compounds, and upon visual examination, 17 compounds were finally selected, purchased, and tested experimentally. Four out of the 17 showed activity against MGMT, and were further analyzed by means of molecular dynamic simulations in explicit solvent (see Materials and Methods). For these four compounds, the commonly employed MMGBSA method to estimate free energy of binding from molecular dynamic trajectories was used. CDOCK binding energies for all the 17 compounds, MMGBSA binding energies for the four more active compounds, together with other chemical and physicochemical properties of the molecules, as stored in the ZINC database,[46] are shown in Table 1. In addition, interaction energy analysis between ligand and the more relevant residues in the binding site were computed (with MMGBSA) and are contained in Table 2.

**MGMT in Vitro Assays.** The 17 top-ranked compounds selected from the VS computations where purchased and

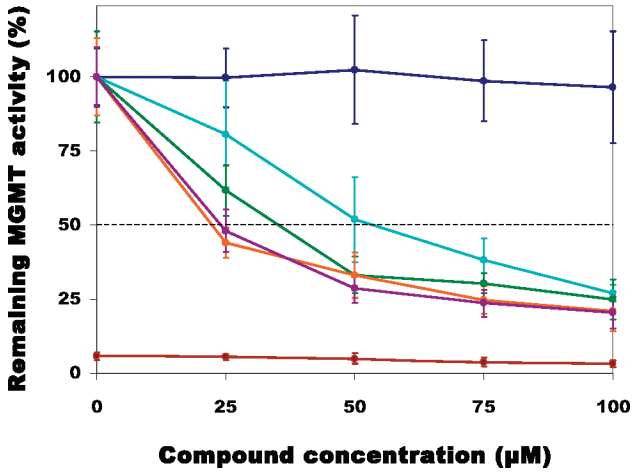


**Figure 3.** Concentration curve showing the inactivation of human alkyltransferase by compounds **1**, **2**, **3**, and **4**. Remaining MGMT activity vs compound concentration is shown relative to untreated control samples. Compounds **1** (cyan), **2** (green), **3** (orange), and **4** (violet) show inhibitory effect on MGMT activity in the micromolar range. The negative control (inactive C145S MGMT protein) is shown in brown, and the effect of the compound solvent (DMSO) on MGMT activity is shown in blue. The dotted line marks the 50% remaining MGMT activity.

dissolved in DMSO. The ability of those 17 candidates to inhibit the recombinant MGMT activity in vitro was determined by measuring the radioactivity transfer from $^3$H-methyled DNA to the active site residue Cys145, as described in the Experimental Section. The resultant $IC_{50}$ values obtained in these experiments for all compounds are shown in Table 1 and in Figure 3. It was found that compounds 5 to 17 did not exhibit significant inhibitor activity in the concentration range used in this assay (Table 1) and therefore were discarded for the subsequent in vivo assays (see below). On the other hand, compounds 1, 2, 3, and 4 inactivated MGMT in the low to medium micromolar range (Figure 3 and Table 1). We checked that MGMT activity was unaffected by any of the solvent (DMSO) volumes used to achieve the desired compound concentration. We did not detect changes, over all the tested compound concentration range, in the remaining radioactivity when an inactive C145S MGMT mutant was used as negative control (Figure 3). The inhibition at 50 $\mu$M compound concentration was not attenuated by addition of 0.001% Triton X-100 or BSA 2 mg/mL (data not shown), confirming that the four compounds were not promiscuous inhibitors.[47,48]

The chemical structures of these compounds are shown in Figure 4. They can be classified into two families according to their chemical architecture. The first family corresponds to quinolinone derivatives 3-[(4-(2,5-dimethylphenyl)-1-piperazinyl)(1-(phenylmethyl)-1*H*-tetrazol-5-il)-methyl]-6-methoxy-2(1*H*)-quinolinone (**1**) and 3-[(4-benzyl-1-piperadinyl)(1-benzyl-1*H*-5-tetrazolyl)]methyl-7-methyl-2(1*H*)-quinolinone (**2**). According to the in vitro activity assays, their affinity values are 54 and 34 $\mu$M, respectively, slightly larger than the affinities obtained for the second family. The second family is composed by triazolo-pyrimidine derivatives 7-(4-(benzyloxy)phenyl)-5-(4-ethylphenyl)-4,5,6,7-tetrahydro-(1,2,4)triazol(1,5-a)pyrimidine (**3**) and 7-(4-(benzyloxy)phenyl)-5-(4-ethoxyphenyl)-4,5,6,7 -tetrahydro-(1,2,4)triazol(1,5-a)pyrimidine (**4**). The corresponding affinities for these compounds are 24 and 22 $\mu$M, respectively.

**MGMT in Vivo Assays.** On the basis of $IC_{50}$ values obtained for the inactivation of pure recombinant MGMT in the in vitro assay, compounds **1**−**4** were further analyzed and validated with in vivo assays. The colony forming assay[49,50] was used in order to study the capability of compounds **1**−**4** to enhance BCNU cytotoxicity using HTB-38 cells. Cells were incubated with these compounds before, during and after BCNU treatment to ensure that inhibitors were present during the entire period of time needed for DNA adducts to be formed. As shown in Figure 5, all four compounds enhance BCNU citotoxicity. BCNU alone reduced the number of colonies by 30%. The cell sensitivity to this chemotherapeutic agent was increased to the 50% when compounds **1**, **3**, and **4** were added at 10 $\mu$M. Only compound **2** needed to be added up to a concentration of 50 $\mu$M to get the same effect. Compound **2** presented little if any sensitizing effect (Figure 5), despite its ability to inhibit MGMT activity in vitro. The ineffectiveness of compound **2** is probably related to a reduced cell penetration. Compound **1** is less effective sensitizing HTB 38 cell to BCNU than compounds **3** and **4**. This is consistent both with their slightly larger in vitro affinity and with their larger log P values. Finally, colony forming experiments have also been carried out in the absence of BCNU, showing an average decrease of 15% using a compound concentration of 50 $\mu$M. These results confirm that cell killing is the final outcome of the joint action between BCNU and the studied compounds.

**Description of the Docking Modes.** The predicted interactions and docking modes of these 4 active compounds, as obtained after docking and molecular dynamics simulations, can be seen in Figure 6. The predicted binding modes suggest that the bound conformation of the inhibitors strongly mimics the observed conformation of the excised, flipped-out nucleotide bearing the damaged base in the complex with MGMT (Figure 6). Thus, the quinolinone fragment of the inhibitors in family 1 (Figure 6A), as well as the alkylphenyl radical of the triazolopyrimidine core in family 2 (Figure 6B), are predicted to occupy the MGMT catalytic cleft, playing the role of analogs of the $O^6$-guanine moiety in the natural substrate, burying deep within the binding groove and reaching the catalytic residue Cys145. In both cases, the remaining portion of the inhibitors is predicted to protrude outside the catalytic pocket and occupy the neighborhood of both the Arg135 and Tyr114. A summary of the most important interactions for each one of the four inhibitors, as computed with the MMGBSA method on the basis of the molecular dynamics simulations, can be found in Table 2. Thus, the tetrazol moiety in family 1 and the triazol group in family 2 are predicted to occupy the site and act as an isosteric group of the 5′ phosphate binding site of the damaged base, adjacent to the active site pocket, and allowing the group to interact with Arg135. This is consistent with the fact that tetrazol groups are well-known isosters of anionic groups, such as carboxylic acids or phosphonates. Similarly, the benzyl-piperazinyl and benzyl-piperadinyl moieties of the inhibitors in family 1, and the benzyloxi-benzyl radical in family 2, are predicted to stack against the aromatic ring of Tyr114. The ranking of the MMGBSA computed average interaction energies correlate well with the observed affinity differences (Table 1), providing some support to the predicted docking modes. Finally, for each complex we computed the most important interactions

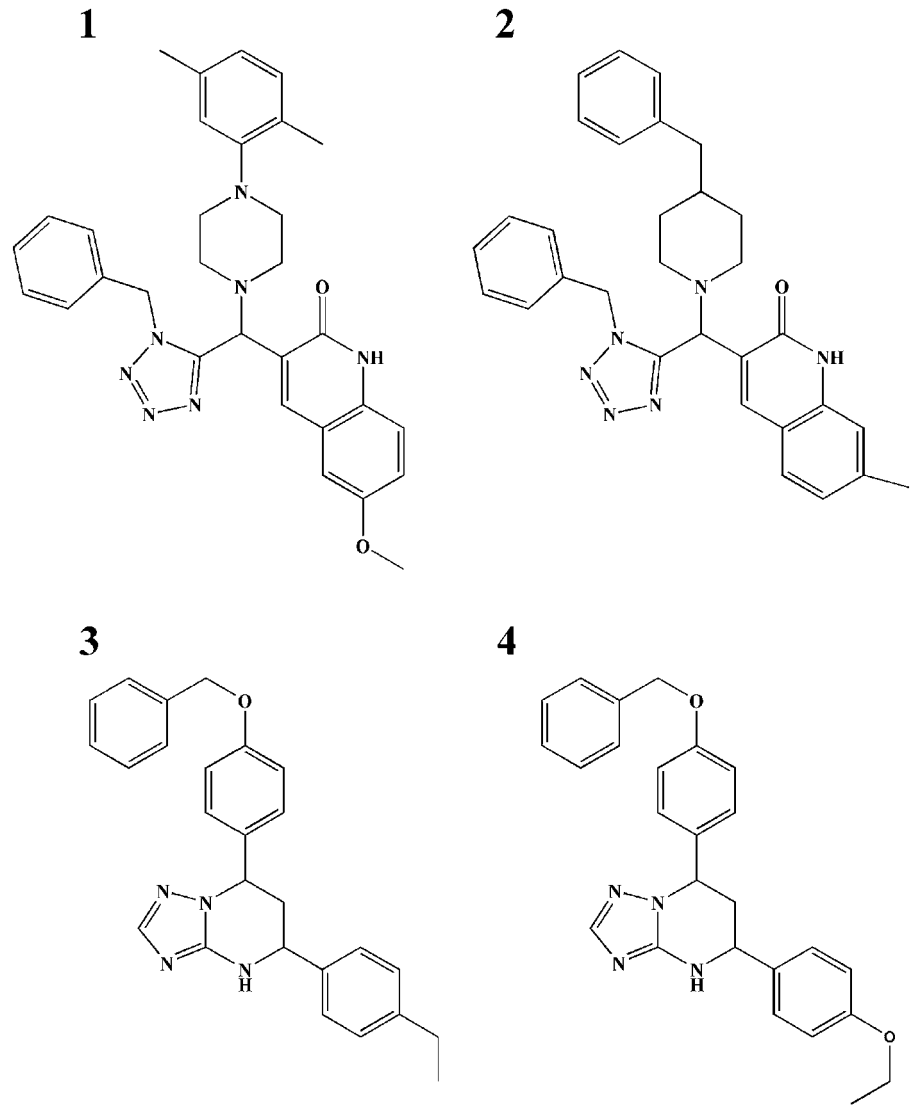


**Figure 4.** Chemical structures of the four compounds that have shown MGMT inhibition in the micro molar range: **1** 3-[(4-(2,5-dimethylphenyl)-1-piperazinyl)(1-(phenylmethyl)-1*H*-tetrazol-5-il)methyl]-6-methoxy-2(1*H*)-quinolinone; **2** 3-[(4-benzyl-1-piperadinyl)(1-benzyl-1*H*-5-tetrazolyl)]methyl-7-methyl-2(1*H*)-quinolinone; **3** 7-(4-(benzyloxy)phenyl)-5-(4-ethylphenyl)-4,5,6,7-tetrahydro-(1,2,4)triazol(1,5-a)pyrimidine; **4** 7-(4-(benzyloxy)phenyl)-5-(4-ethoxyphenyl)-4,5,6,7 -tetrahydro-(1,2,4)triazol(1,5-a)pyrimidine.

between ligand and protein, as obtained from the MMGBSA analysis of the molecular dynamics simulations (Table 2). For all inhibitors the most relevant interactions take place with Arg128 (the arginine finger) and Arg135, as well as Tyr114 and Tyr158. This is consistent with the importance of the residues surrounding the catalytic site as observed in site mutagenesis studies.

## CONCLUSION

We have applied docking and virtual screening techniques to identify novel MGMT inhibitors. Out of 17 inhibitors selected from the ZINC database, four were found to be active. Thus, a success rate of about ~20% for our screening procedure can be estimated. This success rate is consistent with results reported by other groups and highlights the increasingly important role of virtual screening techniques in the search for bioactive molecules. The new compounds belong to two new families of non-nucleosidic inhibitors which, with further optimization, could help to overcome some of the side effects of the existing MGMT inhibitors when combined with alkylating agents. Both families are active in vitro and in vivo in the low to medium micromolar range. The predicted binding modes suggest that the bound conformation of the inhibitors mimics the observed conformation of the flipped-out nucleotide in complex with MGMT. In summary, these novel compounds may form the basis for the development of a new generation of non-nucleosidic MGMT inhibitors with improved pharmacological properties as coadjuvants in cancer chemotherapy.

## EXPERIMENTAL SECTION

**Materials and Methods.** Human colorectal adenocarcinoma cells (ATCC Number HTB-38) were cultured in RPMI 1640 medium (Genycell) supplemented with 10% fetal bovine serum (Biowhittaker). BCNU (1,3-bis-(2-chloroethyl)-1-nitrosourea) was obtained from Sigma and dissolved in 50% phosphate-buffered saline buffer (PBS)−50% ethanol at 4 mM stock solution. *N*-[$^3$H]Methyl-*N*-nitrosourea (MNU) (18.5 MBq/mL, 5 mCi/mL) was purchased from Amersham Biosciences. Candidate compounds were purchased from different companies, in particular compounds **1** and **2** were obtained from Asinex; compounds **3** and **4** were obtained

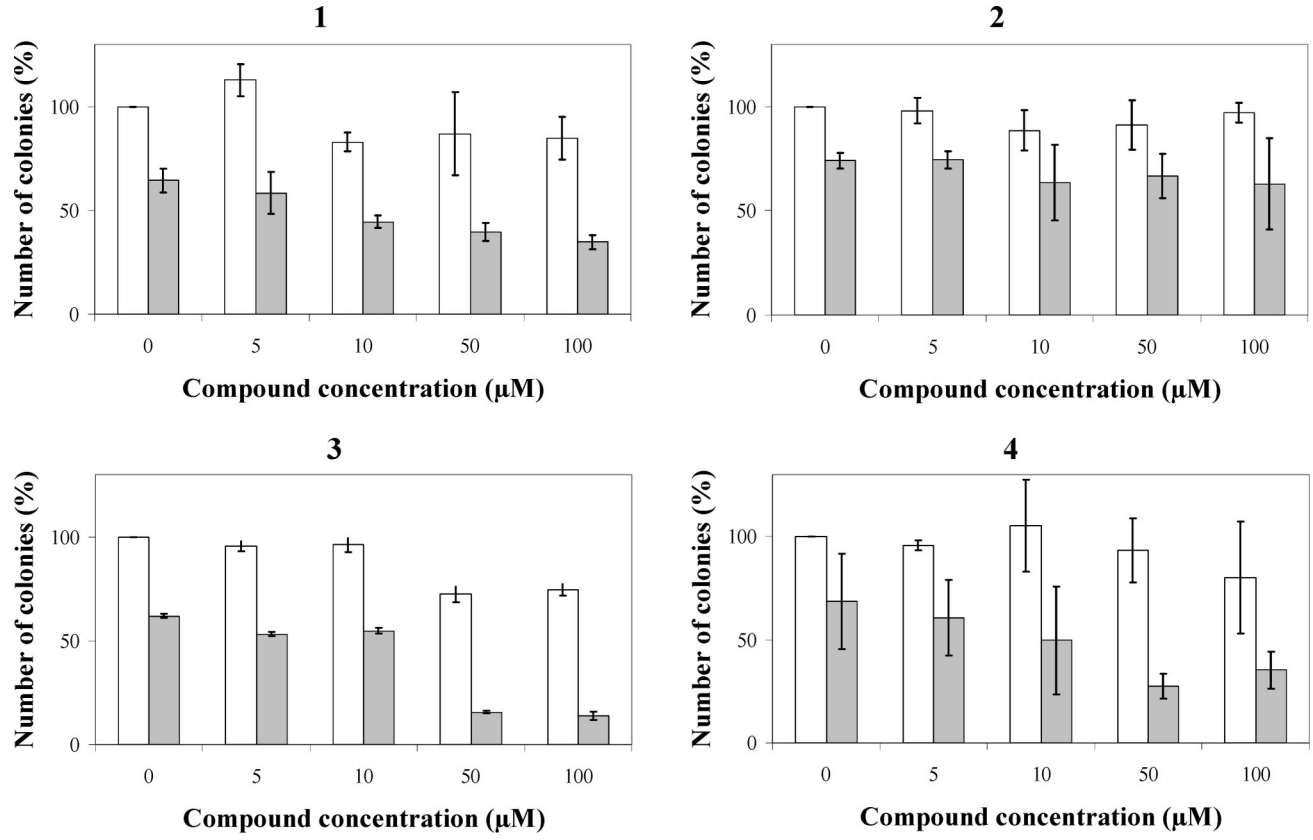


**Figure 5.** Effect of compounds in HTB-38 cells survival, relative to untreated cells. White bars show samples with no BCNU added in the presence of different concentrations of each of the four compounds, and gray bars show the same experiment in the presence of BCNU at 80 $\mu$M. BCNU alone reduce the cell number to an average of 68%; 10, 50, 10, and 100 $\mu$M are the concentrations required to produce 50% cell killing of compounds **1**, **2**, **3**, or **4**, respectively.

from ChemDiv. All of them were dissolved in DMSO (Sigma) at a final concentration of 1 mM and kept at −20 °C until used.

**Virtual Screening (VS).** All VS calculations have been performed within the VSDB platform (to be published, see Figure 1). For clarity, we briefly describe here the main steps comprising the protocol.

*Protein Preparation.* Since no substantial difference appear in the active site among available MGMT structures, we selected the A chain of 1t39[18] (PDB ID code) as receptor. The AMBER8 ff99 force field[51] was then used to assign atom types and charges for each atom in the protein. Hydrogen atoms were added assuming standard protonation states of titratable groups.

*Binding Site Definition and Characterization.* The binding site was built around the cocrystallized ligand (E1X) adding a 5.0 Å *cushion* to the maximum dimensions of the ligand. An equally spaced grid of 0.5 Å was built. In each grid point, the interaction energy of typical atom types (C, N, O, S, P, F, Cl, Br, I, and H) and $e^-$ with all the atoms in the protein were calculated using a combination of 12–6 Lennard-Jones potential and a sigmoidal screening function for van der Waals and electrostatic interactions respectively, with CGRID program.[52] Employing our CDOCK docking program[52] (see below) we docked benzene, water, and methanol molecules generating intermolecular interaction energy maps. Benzene molecule was used here to locate favorable hydrophobic areas, water for hydrophilic sites, and methanol for hydrogen bonds; in a last step the generated energy maps were compressed using GAGA algorithm[42] in form of Gaussian functions trying to capture the most likely areas of interest for each kind of interaction (hydrophobic, hydrophilic, and hydrogen bond). The result of this calculation is the characterization of a sort of negative image of the interaction site. The putative active ligands in the library must conform to this approximate shape.

*Chemical Library Preparation.* Ligands for VS were obtained from the publicly available ZINC database in SMILES format.[53] Multiple protonation states and tautomeric forms are considered as implemented by default in ZINC database. The database was then processed within VSDB as follows: 2D to 3D conversion was carried out with CORINA,[54] up to 6 stereochemical centers were considered, ring conformations generated, hydrogen atoms added, and salt ions removed. Charges were assigned to ligand atoms with MOPAC (MOPAC[55] ESP with MINDO method[56] and radii assignment (AMBER-type[51])). Conformational analysis was carried out with ALFA.[57] ALFA allows the automatic assignment of atom types, detection of rotatable bonds, assignment of possible rotameric states, and generation of conformers. From ZINC we selected around 2.3 million fulfilling the Lipinsky rule of five with up to 7 rotatable bonds.

*Filter 1.* An initial filter was performed with the DOCK program[45] to discard those molecules that do not geometrically fit within the binding site. The spheres needed by DOCK were generated with our algorithm GAGA (see above). 3D molecules were scored with DOCK's contact scoring function. Finally, score values ($score_i$) are converted into Zscore using mean ($\overline{score}$) and standard deviation ($\sigma$)

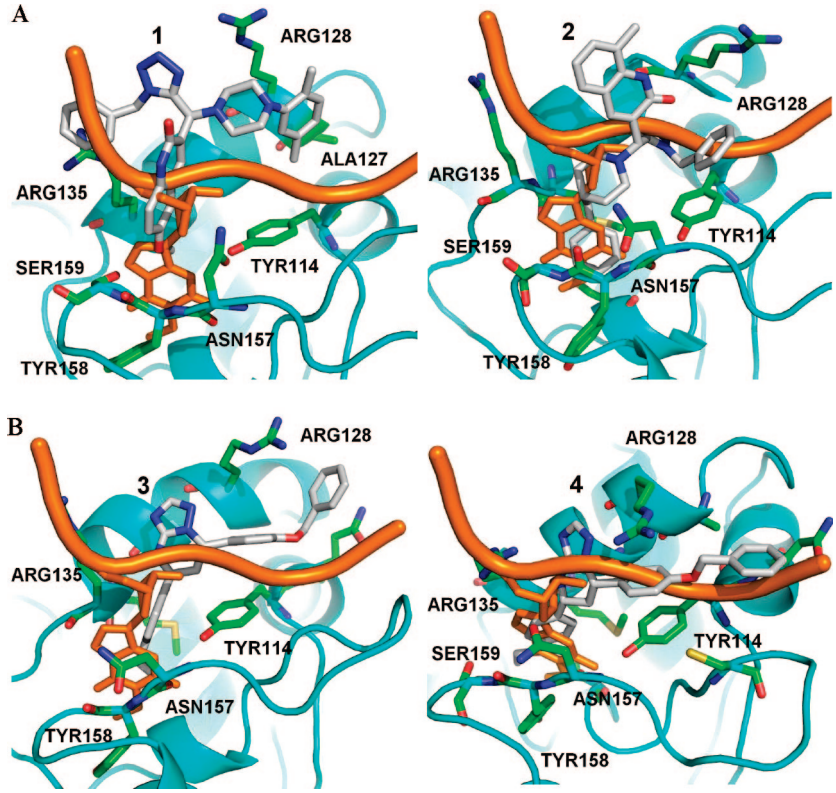


**Figure 6.** Average minimized structure of the compound-MGMT complexes after the molecular dynamics simulations. The structure of the flipped out nucleotide is also shown to highlight the structural similarity between the predicted complexes and the experimental structure. The color code is as follows: the protein is represented as cartoons in cyan; the flipped out nucleotide and part of the DNA backbone is colored in orange; side chains of main interacting residues are colored by atom type: C in green, N in blue, O in red, and S in yellow. The C atoms of compounds **1**−**4** are in gray, and hydrogen atoms are omitted for clarity. A and B correspond to families 1 and 2, respectively, as defined in the Results and Discussion section.

values ($Zscore_i = (score_i - \overline{score})/\sigma$ ). Only molecules with a Zscore beyond the cutoff value of 5 were used to select initial hits. From the initial set of 2.3 million molecules, only 1664 passed the Zscore filter.

*Filter 2.* This last number is an affordable amount of molecules to be studied with a more accurate docking algorithm as CDOCK. CDOCK exhaustively docks each molecule within the binding site using the interaction energy grids calculated with CGRID (see above). The centers of mass of the molecules are positioned on grid points equally spaced 1 Å where discrete rotations of 27° arc on each axel are performed. The "docking energy" for each pose (van der Waals and electrostatic) was then calculated using a trilinear interpolation method. CDOCK program has been proved to be accurate in reproducing native-like conformation starting both from X-ray structure[52] or building the structures from scratch.[58]

*Rescoring.* After docking with CDOCK, electrostatic interaction was corrected for desolvation of ligand and receptor by numerically solving Poisson equation using DelPhi.[59] Details of the calculations can be found elsewhere.[60] All molecules were finally ranked according to their corrected interaction energies, namely, van der Waals plus Coulombic term and desolvation values for receptor and ligand. Finally, the non electrostatic part of solvation was calculated assuming a linear relationship with the solvent accessible surface area. No correction was applied to account for conformational entropy.

*Selection of Candidates.* The best 17 molecules were selected upon analyzing the binding energy, the physicochemical properties of the molecule and visualizing the complexes with Pymol[61] purchased and tested experimentally.

**Molecular Dynamics Simulations.** With the 4 active molecules we carried out a 1 ns molecular dynamics simulation. All simulations were performed at a constant pressure and temperature (1 atm and 300 K) with an integration time step of 2 fs. SHAKE[62] was used to constrain all the bonds involving H atoms at their equilibrium distances. Periodic boundary conditions and the Particle Mesh Ewald methods were used to treat long-range electrostatic effects.[63] AMBER-99[51] and TIP3P[64] force-fields were used in all cases. All the trajectories were performed using the AMBER 8 computer program and associated modules.[65] The four starting models corresponded to the CDOCK predicted complexes. The 4 complexes were hydrated by using boxes containing explicit water molecules, optimized, heated (20 ps), and equilibrated (100 ps). After equilibration, MD trajectories were continued for 1 ns.

Effective binding free energies were qualitatively estimated using the MM-GBSA approach.[66] MM-GBSA method approaches free energy of binding as a sum of a molecular mechanics (MM) interaction term, a solvation contribution thorough a generalized Born (GB) model, and a surface area (SA) contribution to account for the non polar part of desolvation. These calculations were performed for each snapshot from the simulations using the appropriate module within AMBER 8 and averaged out.

**Inhibition of MGMT Activity.** *Protein Production and Purification.* In vitro assays were carried out using recombinant MGMT cloned in the pet-21a(+) (Novagen)

vector. The protein was expressed in the *E. coli* strain Rosetta and once the culture reached an $OD_{600}$ value of 0.8 it was induced by adding 1 mM IPTG during 4 h at 30 °C. The pellet from a 3 L culture was disrupted by sonication and centrifuged. The supernatant was filtered, loaded into a HiTrap FF column (GE Healthcare) and eluted with an Imidazole (Fluka) gradient. Finally the protein was loaded into a Superdex 75 16/60 column (GE Healthcare) being the buffer 150 mM NaCl, 10 mM DTT (Sigma) and 0,1 mM EDTA. The protein was concentrated in this buffer and kept at −20 °C in presence of 40% glycerol. The same protocol has been used for the purification of the inactive mutant MGMT-C145S, cloned in the pet-28a(+) vector (Novagen) and expressed in the *E. coli* strain BL21.

*Substrate Preparation.* The $^3$H-methylation of DNA has been described by Bodgen et al.[67] Briefly, calf thymus DNA (Sigma) was dissolved in 10 mM Sodium Cacodylate pH 7 buffer at 1 mg/mL stock solution. A 7 $\mu$L portion of MNU was added to 1 mL of the DNA stock solution and was then incubated at 37 °C during 2 h. The DNA was precipitated by adding sodium acetate, to a final concentration of 25 mM, and two volumes of cold ethanol 96%. After centrifugation, the DNA pellet was washed twice with cold ethanol, dried, and redissolved overnight at 4 °C in 0.15 N sodium chloride−0.015 N sodium citrate, pH 7.0. The DNA was reprecipitated, washed and dried as described above, redissolved in the reaction buffer (50 mM Tris pH 7, 8; 1 mM DTT; 5 mM EDTA) and stored at −20 °C until use.

*AGT Activity Assay.* The in vitro alkyltransferase activity assay has been previously described.[11,68] Purified protein was incubated with a defined concentration of compound in the reaction buffer at 37 °C. After 30 min [$^3$H]-methylated DNA was added, and the incubation was continued for an additional 90 min. The final volume was 200 $\mu$L, being the DNA concentration 100 times higher than the protein. The reaction was stopped by the addition of 400 $\mu$l of 13% trichloroacetic acid (TCA). DNA was then hydrolyzed by heating the sample at 95 °C for 30 min. The precipitated protein was washed twice with TCA 4% and redissolved in 0.2 M Tris pH 8. The activity corresponding to the [$^3$H]Methyl group transferred to the protein was analyzed by liquid scintillation counting using the Optiphase HiSafe 3 cocktail (Perkin-Elmer) and a Wallac 1414 liquid scintillation analyzer (GMI Inc.). Each compound concentration was assayed in quadruplicate and experiments repeated two times. Percent inhibition was calculated relative to untreated control samples. The $IC_{50}$ values were determined graphically from plots of percent inhibition vs inhibitor concentration.

*Cell Culture Cytotoxic Assay.* The effect of compounds **1**−**4** on the sensitivity of HTB-38 cells to BCNU was determined using colony forming assays as has been described previously in MGMT inhibition studies.[49,50] HTB-38 cells were seeded at $15 \times 10^3$ cells per well density in 6-well, flat-bottomed plates (Falcon) and incubated in a humidified, 5% $CO_2$ incubator at 37 °C for 48 h. Compound solutions were diluted in the culture medium at final concentrations of 100, 50, 10 and 5 $\mu$M, and were immediately used to treat the cells. Cells were incubated with these compounds solutions for 6 h and then BCNU (or the equivalent volume of the vehicle) was added to a final concentration of 80 $\mu$M. After 2 h incubation the medium was replaced with fresh medium containing same compound concentration, and cells were left to grow for an additional 16 h. The cells were then replated at densities of 2000 cells per well in 6-well plates and grown for 12 days until discrete colonies were formed. Colonies were washed twice with PBS and stained with a 0.5% crystal violet−20% ethanol solution. Cells were rinsed with deionized water and air-dried. Finally crystal violet was solubilized with 10% acetic acid solution and the absorbance was measured in a Benchmark Microplate Reader (Bio-Rad). Samples were assayed in duplicate and experiments repeated three times. The percent of remaining cells was calculated relative to untreated control samples.

## ACKNOWLEDGMENT

Work was partially supported by a grant from the "Comunidad de Madrid" (SBIO-0214-2006). Work at CNIO was supported by grants from "Fondo de Investigaciones Sanitarias" FIS (PI030989) and the Education and Science Ministry of Spain (GEN2003-20642-C09-02/NAC). Work at CBMSO was supported by grants from the Education and Science Ministry of Spain (BIO2005-0576 and GEN2003-206420-C09-08), Comunidad de Madrid (200520M157), and by an institutional grant from the Ramón Areces Foundation. Generous allocation of computer time at the Barcelona Supercomputing Center is gratefully acknowledged. C.F. was supported by Fondo de Investigaciones Sanitarias, Ministerio de Sanidad y Consumo (Spain). We thank Dr. Susana Gonzalez for providing HTB-38 cells.

## REFERENCES AND NOTES

(1) Middleton, M. R.; Margison, G. P. Improvement of chemotherapy efficacy by inactivation of a DNA-repair pathway. *Lancet Oncol.* **2003**, *4*, 37–44.

(2) Friedberg, E. C.; Walker, G. C. *DNA Repair and Mutagenesis*, 1st ed.; American Society for Microbiology: Washington, DC, 1995; p 32–33.

(3) Bren, U.; Zupan, M.; Guengerich, F. P.; Mavri, J. Chemical reactivity as a tool to study carcinogenicity: reaction between chloroethylene oxide and guanine. *J. Org. Chem.* **2006**, *71*, 4078–4084.

(4) Bren, U.; Guengerich, F. P.; Mavri, J. Guanine alkylation by the potent carcinogen aflatoxin B1: quantum chemical calculations. *Chem. Res. Toxicol.* **2007**, *20*, 1134–1140.

(5) McMurry, T. B. MGMT inhibitors—The Trinity College-Paterson Institute experience, a chemist's perception. *DNA Repair (Amst)* **2007**, *6*, 1161–1169.

(6) Tong, W. P.; Kirk, M. C.; Ludlum, D. B. Formation of the cross-link 1-[N3-deoxycytidyl),2-[N1-deoxyguanosinyl]ethane in DNA treated with N,N′-bis(2-chloroethyl)-N-nitrosourea. *Cancer Res.* **1982**, *42*, 3102–3105.

(7) Yan, L.; Donze, J. R.; Liu, L. Inactivated MGMT by O6-benzylguanine is associated with prolonged G2/M arrest in cancer cells treated with BCNU. *Oncogene* **2005**, *24*, 2175–2183.

(8) Brent, T. P.; Houghton, P. J.; Houghton, J. A. O6-Alkylguanine-DNA alkyltransferase activity correlates with the therapeutic response of human rhabdomyosarcoma xenografts to 1-(2-chloroethyl)-3-(trans-4-methylcyclohexyl)-1-nitrosourea. *Proc. Natl. Acad. Sci.* **1985**, *82*, 2985–2989.

(9) Tagliabue, G.; Citti, L.; Massazza, G.; Damia, G.; Giavazzi, R.; D'Incalci, M. Tumour levels of O6-alkylguanine-DNA-alkyltransferase and sensitivity to BCNU of human xenografts. *Anticancer Res.* **1992**, *12*, 2123–2125.

(10) Pepponi, R.; Marra, G.; Fuggetta, M. P.; Falcinelli, S.; Pagani, E.; Bonmassar, E.; Jiricny, J.; D'Atri, S. The effect of O6-alkylguanine-DNA alkyltransferase and mismatch repair activities on the sensitivity of human melanoma cells to Temozolomide, 1,3-bis(2-chloroethyl)1-nitrosourea, and cisplatin. *J. Pharmacol. Exp. Ther.* **2003**, *304*, 661–668.

(11) Mattern, J.; Eichhorn, U.; Kaina, B.; Volm, M. O6-methylguanine-DNA methyltransferase activity and sensitivity to cyclophosphamide and cisplatin in human lung tumor xenografts. *Int. J. Cancer* **1998**, *77*, 919–922.

(12) Margison, G. P.; Povey, A. C.; Kaina, B.; Santibanez Koref, M. F. Variability and regulation of O6-alkylguanine-DNA alkyltransferase. *Carcinogenesis* **2003**, *24*, 625–635.
(13) Gerson, S. L. MGMT: its role in cancer aetiology and cancer therapeutics. *Nat. Rev. Cancer* **2004**, *4*, 296–307.
(14) Gerson, S. L. Clinical relevance of MGMT in the treatment of cancer. *J. Clin. Oncol* **2002**, *20*, 2388–2399.
(15) Hegi, M. E.; Diserens, A. C.; Gorlia, T.; Hamou, M. F.; de Tribolet, N.; Weller, M.; Kros, J. M.; Hainfellner, J. A.; Mason, W.; Mariani, L.; Bromberg, J. E.; Hau, P.; Mirimanoff, R. O.; Cairncross, J. G.; Janzer, R. C.; Stupp, R. MGMT gene silencing and benefit from Temozolomide in glioblastoma. *N. Engl. J. Med.* **2005**, *352*, 997–1003.
(16) Esteller, M.; Garcia-Foncillas, J.; Andion, E.; Goodman, S. N.; Hidalgo, O. F.; Vanaclocha, V.; Baylin, S. B.; Herman, J. G. Inactivation of the DNA-repair gene MGMT and the clinical response of gliomas to alkylating agents. *N. Engl. J. Med.* **2000**, *343*, 1350–1354.
(17) Daniels, D. S.; Woo, T. T.; Luu, K. X.; Noll, D. M.; Clarke, N. D.; Pegg, A. E.; Tainer, J. A. DNA binding and nucleotide flipping by the human DNA repair protein AGT. *Nat. Struct. Mol. Biol.* **2004**, *11*, 714–720.
(18) Daniels, D. S.; Mol, C. D.; Arvai, A. S.; Kanugula, S.; Pegg, A. E.; Tainer, J. A. Active and alkylated human AGT structures: a novel zinc site, inhibitor and extrahelical base binding. *EMBO J.* **2000**, *19*, 1719–1730.
(19) Kanugula, S.; Goodtzova, K.; Edara, S.; Pegg, A. E. Alteration of arginine-128 to alanine abolishes the ability of human O6-alkylguanine-DNA alkyltransferase to repair methylated DNA but has no effect on its reaction with O6-benzylguanine. *Biochemistry* **1995**, *34*, 7113–7119.
(20) Mishina, Y.; Duguid, E. M.; He, C. Direct reversal of DNA alkylation damage. *Chem. Rev.* **2006**, *106*, 215–232.
(21) Rasimas, J. J.; Dalessio, P. A.; Ropson, I. J.; Pegg, A. E.; Fried, M. G. Active-site alkylation destabilizes human O6-alkylguanine DNA alkyltransferase. *Protein Sci.* **2004**, *13*, 301–305.
(22) Srivenugopal, K. S.; Yuan, X. H.; Friedman, H. S.; Ali-Osman F. Ubiquitination-dependent proteolysis of O6-methylguanine-DNA methyltransferase in human and murine tumor cells following inactivation with O6-benzylguanine or 1,3-bis(2-chloroethyl)-1-nitrosourea. *Biochemistry* **1996**, *35*, 1328–1334.
(23) Xu-Welliver, M.; Pegg, A. E. Degradation of the alkylated form of the DNA repair protein, O(6)-alkylguanine-DNA alkyltransferase. *Carcinogenesis* **2002**, *23*, 823–830.
(24) Dolan, M. E.; Moschel, R. C.; Pegg, A. E. Depletion of mammalian O6-alkylguanine-DNA alkyltransferase activity by O6-benzylguanine provides a means to evaluate the role of this protein in protection against carcinogenic and therapeutic alkylating agents. *Proc. Natl. Acad. Sci.* **1990**, *87*, 5368–5372.
(25) Pegg, A. E.; Boosalis, M.; Samson, L.; Moschel, R. C.; Byers, T. L.; Swenn, K.; Dolan, M. E. Mechanism of inactivation of human O6-alkylguanine-DNA alkyltransferase by O6-benzylguanine. *Biochemistry* **1993**, *32*, 11998–12006.
(26) Xu-Welliver, M.; Kanugula, S.; Pegg, A. E. Isolation of human O6-alkylguanine-DNA alkyltransferase mutants highly resistant to inactivation by O6-benzylguanine. *Cancer Res.* **1998**, *58*, 1936–1945.
(27) Pegg, A. E.; Swenn, K.; Chae, M. Y.; Dolan, M. E.; Moschel, R. C. Increased killing of prostate, breast, colon, and lung tumor cells by the combination of inactivators of O6-alkylguanine-DNA alkyltransferase and N,N′-bis(2-chloroethyl)-N-nitrosourea. *Biochem. Pharmacol.* **1995**, *50*, 1141–1148.
(28) Kreklau, E. L.; Kurpad, C.; Williams, D. A.; Erickson, L. C. Prolonged inhibition of O(6)-methylguanine DNA methyltransferase in human tumor cells by O(6)-benzylguanine in vitro and in vivo. *J. Pharmacol. Exp. Ther.* **1999**, *291*, 1269–1275.
(29) Rabik, C. A.; Njoku, M. C.; Dolan, M. E. Inactivation of O6-alkylguanine DNA alkyltransferase as a means to enhance chemotherapy. *Cancer Treat. Rev.* **2006**, *32*, 261–276.
(30) Dolan, M. E.; Chae, M. Y.; Pegg, A. E.; Mullen, J. H.; Friedman, H. S.; Moschel, R. C. Metabolism of O6-benzylguanine, an inactivator of O6-alkylguanine-DNA alkyltransferase. *Cancer Res.* **1994**, *54*, 5123–5130.
(31) Schilsky, R. L.; Dolan, M. E.; Bertucci, D.; Ewesuedo, R. B.; Vogelzang, N. J.; Mani, S.; Wilson, L. R.; Ratain, M. J. Phase I clinical and pharmacological study of O6-benzylguanine followed by carmustine in patients with advanced cancer. *Clin. Cancer Res.* **2000**, *6*, 3025–3031.
(32) Gajewski, T. F.; Sosman, J.; Gerson, S. L.; Liu, L.; Dolan, E.; Lin, S.; Vokes, E. E. Phase II trial of the O6-alkylguanine DNA alkyltransferase inhibitor O6-benzylguanine and 1,3-bis(2-chloroethyl)-1-nitrosourea in advanced melanoma. *Clin. Cancer Res.* **2005**, *11*, 7861–7865.
(33) Bacolod, M. D.; Johnson, S. P.; Pegg, A. E.; Dolan, M. E.; Moschel, R. C.; Bullock, N. S.; Fang, Q.; Colvin, O. M.; Modrich, P.; Bigner, D. D.; Friedman, H. S. Brain tumor cell lines resistant to O6-benzylguanine/1,3-bis(2-chloroethyl)-1-nitrosourea chemotherapy have O6-alkylguanine-DNA alkyltransferase mutations. *Mol. Cancer Ther.* **2004**, *3*, 1127–1135.
(34) Liu, L.; Schwartz, S.; Davis, B. M.; Gerson, S. L. Chemotherapy-induced O(6)-benzylguanine-resistant alkyltransferase mutations in mismatch-deficient colon cancer. *Cancer Res.* **2002**, *62*, 3070–3076.
(35) Phillips, W. P., Jr.; Gerson, S. L. Acquired resistance to O6-benzylguanine plus chloroethylnitrosoureas in human breast cancer. *Cancer Chemother. Pharmacol.* **1999**, *44*, 319–326.
(36) Ranson, M.; Middleton, M. R.; Bridgewater, J.; Lee, S. M.; Dawson, M.; Jowle, D.; Halbert, G.; Waller, S.; McGrath, H.; Gumbrell, L.; McElhinney, R. S.; Donnelly, D.; McMurry, T. B.; Margison, G. P. Lomeguatrib, a potent inhibitor of O6-alkylguanine-DNA-alkyltransferase: phase I safety, pharmacodynamic, and pharmacokinetic trial and evaluation in combination with Temozolomide in patients with advanced solid tumors. *Clin. Cancer. Res.* **2006**, *12*, 1577–1584.
(37) Stoermer, M. J. Current status of virtual screening as analysed by target class. *Med. Chem.* **2006**, *2*, 89–112.
(38) Klebe, G. Virtual ligand screening: strategies, perspectives and limitations. *Drug Discov. Today* **2006**, *11*, 580–594.
(39) Warren, G. L.; Andrews, C. W.; Capelli, A. M.; Clarke, B.; LaLonde, J.; Lambert, M. H.; Lindvall, M.; Nevins, N.; Semus, S. F.; Senger, S.; Tedesco, G.; Wall, I. D.; Woolven, J. M.; Peishoff, C. E.; Head, M. S. A critical assessment of docking programs and scoring functions. *J. Med. Chem.* **2006**, *49*, 5912–5931.
(40) Michel, J.; Verdonk, M. L.; Essex, J. W. Protein-ligand binding affinity predictions by implicit solvent simulations: a tool for lead optimization. *J. Med. Chem.* **2006**, *49*, 7427–7439.
(41) Weis, A.; Katebzadeh, K.; Soderhjelm, P.; Nilsson, I.; Ryde, U. Ligand affinities predicted with the MM/PBSA method: dependence on the simulation method and the force field. *J. Med. Chem.* **2006**, *49*, 6596–6606.
(42) Kollman, P. A.; Massova, I.; Reyes, C.; Kuhn, B.; Huo, S.; Chong, L.; Lee, M.; Lee, T.; Duan, Y.; Wang, W.; Donini, O.; Cieplak, P.; Srinivasan, J.; Case, D. A.; Cheatham, T. E., 3rd. Calculating structures and free energies of complex molecules: combining molecular mechanics and continuum models. *Acc. Chem. Res.* **2000**, *33*, 889–897.
(43) Massova, I.; Kollman, P. A. Combined molecular mechanical and continuum solvent approach (MM-PBSA/GBSA) to predict ligand binding. *Perspect. Drug Discov. Des.* **2000**, *200*, 113–135.
(44) Aqvist, J.; Medina, C.; Samuelsson, J. E. A new method for predicting binding affinity in computer-aided drug design. *Protein Eng.* **1994**, *7*, 385–391.
(45) Kuntz, I. D.; Blaney, J. M.; Oatley, S. J.; Langridge, R.; Ferrin, T. E. A geometric approach to macromolecule-ligand interactions. *J. Mol. Biol.* **1982**, *161*, 269–288.
(46) Irwin, J. J.; Shoichet, B. K. ZINC—a free database of commercially available compounds for virtual screening. *J. Chem. Inf. Model.* **2005**, *45*, 177–182.
(47) McGovern, S. L.; Caselli, E.; Grigorieff, N.; Shoichet, B. K. A common mechanism underlying promiscuous inhibitors from virtual and high-throughput screening. *J. Med. Chem.* **2002**, *45*, 1712–1722.
(48) McGovern, S. L.; Helfand, B. T.; Feng, B.; Shoichet, B. K. A specific mechanism of nonspecific inhibition. *J. Med. Chem.* **2003**, *46*, 4265–4272.
(49) Pegg, A. E.; Goodtzova, K.; Loktionova, N. A.; Kanugula, S.; Pauly, G. T.; Moschel, R. C. Inactivation of human O(6)-alkylguanine-DNA alkyltransferase by modified oligodeoxyribonucleotides containing O(6)-benzylguanine. *J. Pharmacol. Exp. Ther.* **2001**, *296*, 958–965.
(50) Nelson, M. E.; Loktionova, N. A.; Pegg, A. E.; Moschel, R. C. 2-amino-O4-benzylpteridine derivatives: potent inactivators of O6-alkylguanine-DNA alkyltransferase. *J. Med. Chem.* **2004**, *47*, 3887–3891.
(51) Cornell, W. D.; Cieplak, P.; Bayly, C. I.; Gould, I. R.; Merz, K. M.; Ferguson, D. M.; Spellmeyer, D. C.; Fox, T.; Caldwell, J. W.; Kollman, P. A. A Second Generation Force Field for the Simulation of Proteins, Nucleic Acids, and Organic Molecules. *J. Am. Chem. Soc.* **1995**, *117*, 5179–5197.
(52) Perez, C.; Ortiz, A. R. Evaluation of docking functions for protein-ligand docking. *J. Med. Chem.* **2001**, *44*, 3768–3785.
(53) Weininger, D. SMILES, a Chemical Language and Information System. 1. Introduction to Methodology and Encoding Rules. *J. Chem. Inf. Comput. Sci.* **1988**, *28*, 31–36.
(54) *Corina Molecular Networks*; GmbH Computerchemie: Germany, 2000.
(55) Stewart, J. J. MOPAC: a semiempirical molecular orbital program. *J. Comput. Aided Mol. Des.* **1990**, *4*, 1–105.
(56) Dewar, M. J. S.; Thiel, W. MIND0/3 Study of the Addition of Singlet Oxygen (1deltagO2) to 1,3-Butadiene. *J. Am. Chem. Soc.* **1977**, *99*, 2338–2339.
(57) Gil-Redondo, R. Implementación de una plataforma para el cribado virtual de quimiotecas. Master Thesis; Universidad Nacional de Educación a Distancia, Madrid, Spain, 2006.

(58) Murcia, M.; Morreale, A.; Ortiz, A. R. Comparative binding energy analysis considering multiple receptors: a step toward 3D-QSAR models for multiple targets. *J. Med. Chem.* **2006**, *49*, 6241–6253.
(59) Rocchia, W.; Sridharan, S.; Nicholls, A.; Alexov, E.; Chiabrera, A.; Honig, B. Rapid grid-based construction of the molecular surface and the use of induced surface charge to calculate reaction field energies: applications to the molecular systems and geometric objects. *J. Comput. Chem.* **2002**, *23*, 128–137.
(60) Morreale, A.; Gil-Redondo, R.; Ortiz, A. R. A new implicit solvent model for protein-ligand docking. *Proteins* **2007**, *67*, 606–616.
(61) DeLano, W. L. *The PyMOL Molecular Graphics System* DeLano Scientific: Palo Alto, CA, 2002.
(62) Ryckaert, J.; Ciccotti, G.; Berendsen, H. Numerical Integration of the Cartesian Equations of Motion of a System with Constraints: Molecular Dynamics of n-Alkanes. *J. Comp. Phys.* **1977**, *23*, 327–341.
(63) Darden, T.; York, D.; Pedersen, L. Particle mesh Ewald: An N·log(N) method for Ewald sums in large systems. *J. Chem. Phys.* **1993**, *98*, 10089–10092.
(64) Jorgensen, W.; Chandrasekhar, J.; Madura, J.; Impey, R.; Klein, M. Comparison of simple potential functions for simulating liquid water. *J. Chem. Phys.* **1983**, *79*, 926–935.
(65) McGovern, S. L.; Caselli, E.; Grigorieff, N.; Shoichet, B. K. A common mechanism underlying promiscuous inhibitors from virtual and high-throughput screening. *J. Med. Chem.* **2002**, *45*, 1712–1722.
(66) Still, W.; Tempczyk, A.; Hawley, R.; Hendrickson, T. Semianalytical treatment of solvation for molecular mechanics and dynamics. *J. Am. Chem. Soc.* **1990**, *112*, 6127–6129.
(67) Bogden, J. M.; Eastman, A.; Bresnick, E. A system in mouse liver for the repair of O6-methylguanine lesions in methylated DNA. *Nucleic Acids Res.* **1981**, *9*, 3089–3103.
(68) Reinhard, J.; Hull, W. E.; von der Lieth, C. W.; Eichhorn, U.; Kliem, H. C.; Kaina, B.; Wiessler, M. Monosaccharide-linked inhibitors of O(6)-methylguanine-DNA methyltransferase (MGMT): synthesis, molecular modeling, and structure-activity relationships. *J. Med. Chem.* **2001**, *44*, 4050–4061.

CI700447R